Motion analysis of optically trapped particles and cells using 2D Fourier analysis

Kristensen, Martin Verner; Ahrendt, Peter; Lindballe, Thue Bjerring; Abildgaard, Otto Højager Attermann; Kylling, Anton P.; Karstoft, Henrik; Imparato, Alberto; Hosta-Rigau, Leticia; Stadler, Brigitte; Stapelfeldt, Henrik; Keiding, Søren Rud

Published in:
Optics Express

Link to article, DOI:
10.1364/OE.20.001953

Publication date:
2012

Document Version
Publisher's PDF, also known as Version of record

Motion analysis of optically trapped particles and cells using 2D Fourier analysis

Martin Verner Kristensen,[1] Peter Ahrendt,[2] Thue Bjerring Lindballe,[3] Otto Højager Attermann Nielsen,[4] Anton P. Kylling,[6] Henrik Karstoft,[2] Alberto Imparato,[3] Leticia Hosta-Rigau,[1] Brigitte Stadler,[1] Henrik Stapelfeldt,[1,5] Søren Rud Keiding[1,2,5,*]

[1]*iNANO, Aarhus University, Ny Munkegade, DK-8000 Aarhus C, Denmark*
[2]*Department of Engineering, Aarhus University, Ny Munkegade, DK-8000 Aarhus C. Denmark*
[3]*Department of Physics and Astronomy, Aarhus University, Ny Munkegade, DK-8000 Aarhus C, Denmark*
[4]*DTU-Photonics, Technical University of Denmark, Oersteds Plads, Build. 343, DK-2800 Kgs Lyngby, Denmark*
[5]*Institute of Chemistry, Aarhus University, Langelandsgade 140, DK-8000 Aarhus C, Denmark*
[6]*Unisense Fertilitech, Tueager 1, DK-8200 Aarhus N, Denmark*
[*]*keiding@ase.au.dk*

Abstract: Motion analysis of optically trapped objects is demonstrated using a simple 2D Fourier transform technique. The displacements of trapped objects are determined directly from the phase shift between the Fourier transform of subsequent images. Using end- and side-view imaging, the stiffness of the trap is determined in three dimensions. The Fourier transform method is simple to implement and applicable in cases where the trapped object changes shape or where the lighting conditions change. This is illustrated by tracking a fluorescent particle and a myoblast cell, with subsequent determination of diffusion coefficients and the trapping forces.

OCIS codes: (350.4855) Optical tweezers or optical manipulation; (070.0070) Fourier optics and signal processing; (100.0100) Image processing.

References and links

1. J. Glückstad, "Optical manipulation sculpting the object," Nat. Photonics **5**(1), 7–8 (2011).
2. D. G. Grier, "A revolution in optical manipulation," Nature **424**(6950), 810–816 (2003).
3. F. C. Cheong, B. J. Krishnatreya, and D. G. Grier, "Strategies for three-dimensional particle tracking with holographic video microscopy," Opt. Express **18**(13), 13563–13573 (2010).
4. J. Fung, K. E. Martin, R. W. Perry, D. M. Kaz, R. McGorty, and V. N. Manoharan, "Measuring translational, rotational, and vibrational dynamics in colloids with digital holographic microscopy," Opt. Express **19**(9), 8051–8065 (2011).
5. O. Otto, F. Czerwinski, J. L. Gornall, G. Stober, L. B. Oddershede, R. Seidel, and U. F. Keyser, "Real-time particle tracking at 10,000 fps using optical fiber illumination," Opt. Express **18**(22), 22722–22733 (2010).
6. R. Bowman, G. Gibson, and M. Padgett, "Particle tracking stereomicroscopy in optical tweezers: control of trap shape," Opt. Express **18**(11), 11785–11790 (2010).
7. J. Guck, R. Ananthakrishnan, H. Mahmood, T. J. Moon, C. C. Cunningham, and J. Käs, "The optical stretcher: a novel laser tool to micromanipulate cells," Biophys. J. **81**(2), 767–784 (2001).
8. B. S. Reddy and B. N. Chatterji, "An FFT-based technique for translation, rotation, and scale-invariant image registration," IEEE Trans. Image Process. **5**(8), 1266–1271 (1996).
9. J. P. Staforelli, E. Vera, J. M. Brito, P. Solano, S. Torres, and C. Saavedra, "Superresolution imaging in optical tweezers using high-speed cameras," Opt. Express **18**(4), 3322–3331 (2010).
10. M. Guizar-Sicairos, S. T. Thurman, and J. R. Fienup, "Efficient subpixel image registration algorithms," Opt. Lett. **33**(2), 156–158 (2008).
11. C. D. Kuglin and D. C. Hines, "The phase correlation image alignment method," Proc. Int. Conf. Cybernetics Society **163–5** (1975).
12. D. Palima and J. Glückstad, "Generalised phase contrast: microscopy, manipulation and more," Contemp. Phys. **51**(3), 249–265 (2010).
13. T. B. Lindballe, M. V. Kristensen, A. P. Kylling, D. Z. Palima, J. Glückstad, S. R. Keiding, and H. Stapelfeldt, "Three-dimensional imaging and force characterization of multiple trapped particles in low NA counterpropagating optical traps," J. Eur. Opt. Soc-Rapid. **6**, 110576 (2011).
14. P. J. Rodrigo, I. R. Perch-Nielsen, C. A. Alonzo, and J. Glückstad, "GPC-based optical micromanipulation in 3D real-time using a single spatial light modulator," Opt. Express **14**(26), 13107–13112 (2006).
15. K. C. Neuman and S. M. Block, "Optical trapping," Rev. Sci. Instrum. **75**(9), 2787–2809 (2004).
16. H. S. Stone, M. T. Orchard, E. C. Chang, and S. A. Martucci, ""A fast direct Fourier-based algorithm for subpixel registration of images," IEEE T Geosci. Remote **39**(10), 2235–2243 (2001).

#158777 - $15.00 USD Received 23 Nov 2011; revised 2 Jan 2012; accepted 2 Jan 2012; published 13 Jan 2012

17. M. Balci and H. Foroosh, "Subpixel estimation of shifts directly in the Fourier domain," IEEE Trans. Image Process. **15**(7), 1965–1972 (2006).
18. T. J. Grassman, M. K. Knowles, and A. H. Marcus, "Structure and dynamics of fluorescently labeled complex fluids by fourier imaging correlation spectroscopy," Phys. Rev. E Stat. Phys. Plasmas Fluids Relat. Interdiscip. Topics **62**(6 6 Pt B), 8245–8257 (2000).
19. K. Berg-Sørensen and H. Flyvbjerg, "Power spectrum analysis for optical tweezers," Rev. Sci. Instrum. **75**(3), 594–612 (2004).
20. S. Pasche, S. M. De Paul, J. Voros, N. D. Spencer, and M. Textor, "Poly(L-lysine)-graft-poly(ethylene glycol) assembled monolayers on niobium oxide surfaces: A quantitative study of the influence of polymer interfacial architecture on resistance to protein adsorption by ToF-SIMS and in situ OWLS," Langmuir **19**(22), 9216–9225 (2003).
21. G. M. Cortelazzo, L. Lucchese, and C. M. Monti, "Frequency domain analysis of general planar rigid motion with finite duration," J. Opt. Soc. Am. A **16**(6), 1238–1253 (1999).

1. Introduction

As optical tweezers and counterpropagating optical traps are gradually becoming standard techniques [1, 2], reliable tracking algorithms are in demand [3–6]. This is particularly true when tracking irregular biological objects where both the shape [7] and the lighting conditions can change during the experiment. In this letter, we demonstrate a technique for sub-pixel tracking of optically trapped objects based on video recordings of their motion. Tracking is achieved through an analysis of the 2D Fourier transform [8–10] of the individual images of the recorded video. The 2D Fourier method described here handles changes in object shape and illumination conditions, as long as the changes are slow compared to the frame rate of the camera. This is in contrast to standard tracking techniques where the shape and illumination must remain unchanged during the image sequence [11].

We illustrate the 2D Fourier transform motion analysis (FTMA) using data obtained from an optical trapping setup based on counterpropagating beams, shaped by the generalized phase contrast method and a spatial light modulator [12]. The large working distance between the objectives (> 10 mm) enables monitoring of the trapped objects from two orthogonal directions with an end-view camera (along the trapping beam direction) and a side-view camera [13, 14] thus obtaining 3D information of the particle motion and the trap stiffness. First, we describe the FTMA method and illustrate its application by measuring the trap stiffness for a 10 μm diameter polystyrene bead under illumination. Second, we show that the method can track a fluorescing polystyrene bead where the illumination changes strongly due to bleaching – an effect that renders standard camera-based tracking methods difficult to apply. Third, we track a myoblast cell, demonstrating that the method also works on irregular objects, a complication that makes standard tracking methods unreliable, including those based on position sensitive detectors, and quadrant photodiodes [11, 15].

2. Theory

2.1. Fourier transform motion analysis

The FTMA method is a well-established technique in image analysis used in, for example, superresolution [16–18]. Assuming, for simplicity, that we have two images of an object, represented by $f_1(x_1,y_1)$ and $f_2(x_2,y_2)$, where the x and y coordinates specify the object's center of mass in the given image. Let any object in the images be equal, except for a linear displacement along the vector $(\Delta x,\Delta y)$, and let the background be flat. Given these restrictions, the two images will be related in the following way

$$f_2\left(x+\Delta x, y+\Delta y\right) = f_1\left(x, y\right). \tag{1}$$

Since the amplitude of the Fourier transform of each image depends only on the shape of the object in the image, and not its position, a simple expression for the displacement can be obtained from the ratio of the Fourier transformed images, $F_1(k_x,k_y)$ and $F_2(k_x,k_y)$

#158777 - $15.00 USD Received 23 Nov 2011; revised 2 Jan 2012; accepted 2 Jan 2012; published 13 Jan 2012

$$\frac{F_2\left(k_x,k_y\right)}{F_1\left(k_x,k_y\right)}=\frac{A\left(k_x,k_y\right)e^{-i\left(k_x\left(x+\Delta x\right)+k_y\left(y+\Delta y\right)\right)}}{A\left(k_x,k_y\right)e^{-i\left(k_x x+k_y y\right)}}=e^{-i\left(k_x\Delta x+k_y\Delta y\right)}=e^{-i\Delta\theta\left(k_x,k_y\right)}. \quad (2)$$

The displacement (Δx,Δy) of the particle from one frame to the next frame is calculated as the slope of the phase plane

$$\Delta\theta\left(k_x,k_y\right)=\Delta x k_x+\Delta y k_y. \quad (3)$$

The slope is computed using a least mean square fit of the phase difference surface. From the 2D experimental values of the phase one can obtain the slope of the phase plane, a vector defined as (Δx,Δy), and the intercept of the phase plane with the k_x and k_y axes using linear regression. The motion of the object can subsequently be analyzed using the displacement measured between consecutive frames. Appropriate threshold filters should be applied, depending on the signal to noise ratio of the images, effects of pixelation, missing pixels, and the presence of other unrelated objects in the image or a non-flat background, in order to identify the frequencies specific for the trapped object. We have used a simple filter that removes the DC-component of the image ($k_x = k_y = 0$ μm^{-1}) and subsequently, a threshold filter that suppresses low amplitude frequency noise in the image.

3. Experimental results

3.1. Tracking of a 10 μm polystyrene bead

As a first demonstration of the ability of the FTMA to track particles, we have analyzed the motion of a single 10 μm diameter polystyrene bead in a counterpropagating optical trap. The bead is trapped between the two foci (each with a diameter of 10 μm) of the counterpropagating beams, which are separated by 106 μm. The optical power in each beam of the trap is 3.7 mW and the wavelength is 1065 nm. The particle is imaged both in end-view, showing the motion transversal to the trapping lasers (x,y), and in side-view, showing motion along the z-axis and x-axis. The x-axis is thus observed in both side- and end-view. The frame rate of the cameras was set to 400 Hz with a region of interest (ROI) of 576 × 576 pixels, and the two cameras are synchronized to within 17 nanoseconds. The method used to calibrate the imaging system, as well as more thorough description of the experimental setup, is described in previous work [13]. The motion of the trapped particle is followed for 600 seconds resulting in 240000 frames to be analyzed per camera. Using the FTMA method, we obtain the relative displacement of the particle between two successive frames.

#158777 - $15.00 USD Received 23 Nov 2011; revised 2 Jan 2012; accepted 2 Jan 2012; published 13 Jan 2012

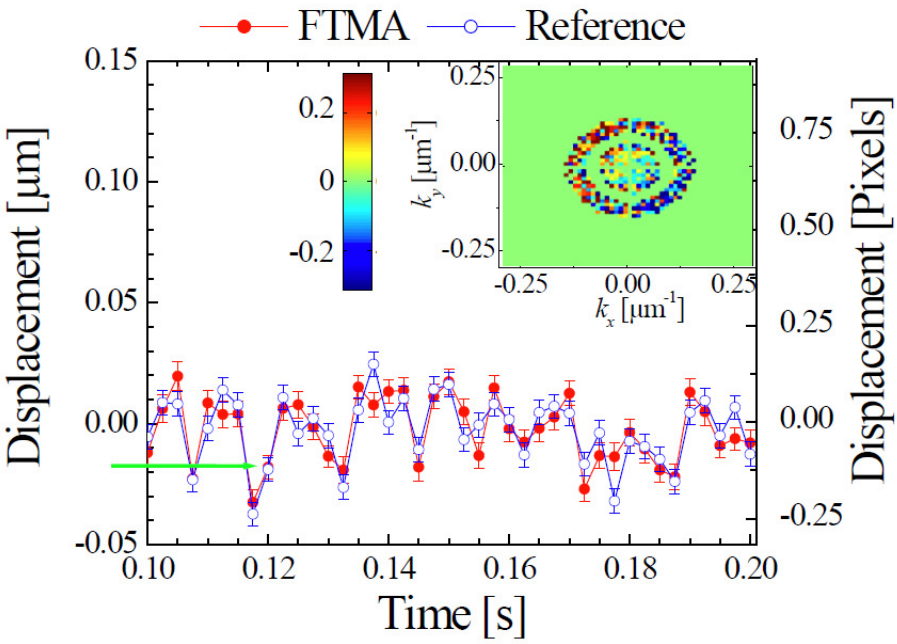

Fig. 1. Comparison of traces of particle displacements along the x-axis obtained through the FTMA method (red) and a reference tracking algorithm (blue). The error bars indicate the uncertainty of the tracking algorithms. The inset shows an example of the phase plane corresponding to the displacement at 0.12 seconds, indicated by the green arrow. The displacement is shown in both µm and pixels. A threshold filter was applied to remove phase data corresponding to low spatial frequencies (DC-components) and spatial frequencies with low spectral amplitude. The phase plane is down-sloped in the x-axis direction indicating a displacement along the negative x-axis

Selected parts of the full track corresponding to the time interval from 0.1 to 0.2 seconds are shown in Fig. 1 as dots. Each red dot corresponds to the Δx-component of the displacement vector $(\Delta x,\Delta y)$ obtained from Eq. (3). The inset shows an example of the phase plane obtained from two consecutive images at 0.12 seconds. The phase plane has a falling slope pointing along the negative k_x-axis as indicated by the change in color from blue to yellow/orange in the inset. The measured displacements correspond to a fraction of a pixel, equivalent to ± 50 nm. In Fig. 1, we compared the FTMA method to a reference tracking algorithm (blue dots) where the particle position is obtained by convoluting each image with a filter function specific to the trapped particle [11]. Subsequently, the displacement is calculated by subtracting neighboring positions. Very good agreement between the two tracking methods is evident from Fig. 1. One can quantify the agreement by first assuming that the displacement obtained by the reference tracking algorithm is exact and then subtracting the displacement obtained from the two methods. This gives a Gaussian distribution centered on zero displacement with a standard deviation σ = 8 nm. The accuracy of the reference tracking method is described in more detail in [13] and is limited by the camera resolution, mechanical drift of the setup and the tracking algorithm. This amounts to an accuracy limited to a standard deviation σ = 5 nm. In the present case, where a simple object is tracked under optimum lightning condition, the accuracy of the FTMA method is thus comparable to that of the reference method. In general, however, the accuracy of both methods is sensitively dependent on the experimental conditions. We have performed numerical tests of the FTMA method, investigating the standard error in determining the slope of the phase plane as function of the signal to noise ration of the image. The slope is directly

#158777 - $15.00 USD Received 23 Nov 2011; revised 2 Jan 2012; accepted 2 Jan 2012; published 13 Jan 2012

proportional to the displacement, and we find that the standard error is inversely proportional to the signal to noise ratio of the image.

From the particle positions obtained by the reference method, we determine the trap stiffness and the diffusion coefficient using the power spectrum method [19] as shown in Fig. 2(a). The results for the x- and y-axis are κ_x = 0.72(1) pN/μm and κ_y = 0.73(1) pN/μm. The trap stiffness along the z-axis is very low (κ_z < 0.1 pN/μm) and will not be considered here. The diffusion coefficient was determined to be D = 0.045(1) μm^{2}s. When the particle is tracked using the FTMA method, we sample the displacement $\Delta = x_{i+1} - x_i$ between two consecutive frames. The sampled displacement refers to the particle's thermal (Brownian) motion inside the trapping potential defined by the two trapping laser beams. By solving the Langevin equation one can show that the Gaussian variance of the displacement is given by

$$\left\langle \Delta^2 \right\rangle = 2D\tau\left(1+\pi\tau f_c\right) \tag{4}$$

where D is the diffusion coefficient given by $D = k_B T/\gamma$, γ is the friction coefficient, k_B is the Boltzmann constant, and T is temperature. τ is the sampling time given by $\tau = 1/fps$, where fps is the frame rate of the camera and f_c is the corner frequency given by $f_c = \kappa/2\pi\gamma$, where κ is the trap stiffness. The first term in Eq. (4) is equal to that of a free particle and the second, in the present case, negligible term is (through the corner frequency) dependent on the trapping potential. Consequently, the trap stiffness is poorly determined from the distribution of the particle displacements.

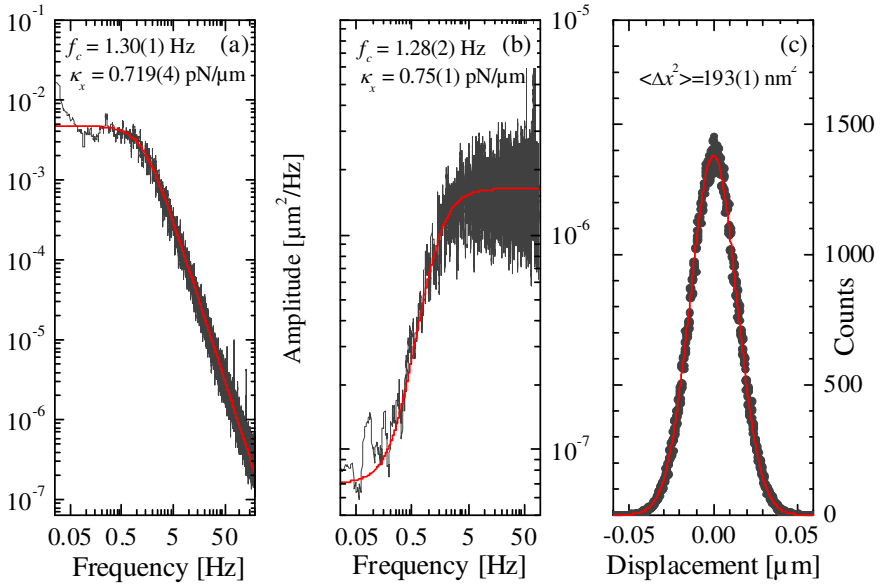

Fig. 2. A reference tracking algorithm (a) and the FTMA method (b) and (c) are used on the same 400 fps movie of a trapped 10 μm polystyrene bead for comparison. (a) Power spectrum of the particle movement (black line). The red line is the fitted power spectrum $|S_x|^2$ (b) Power spectrum for the particle displacement along the x-axis (black line). The red line is the fitted power spectrum of the displacement $|S_{\Delta x}|^2$ as given by Eq. (5). The low frequency noise floor in (b) is 7 × 10^{-8} μm^2/Hz. (c) Histogram showing distribution of displacements along the x-axis (black dots) and the fitted Gaussian distribution. In (a) and (b) sharp noise peaks at 56 and 76 Hz caused by mechanical noise in the laboratory was removed from the data before fitting the power spectra. The experimental data points were averaged (10 point adjacent averaging) before plotting, but after fitting.

#158777 - $15.00 USD Received 23 Nov 2011; revised 2 Jan 2012; accepted 2 Jan 2012; published 13 Jan 2012

The trap stiffness can be determined from the power spectrum of the displacement. The displacement is related to the average velocity between samples and the power spectrum of the displacement is obtained by differentiating the position with respect to time. In frequency space this amounts to multiplying with $(-if)$ for amplitude and $(-f^2)$ for power. In addition, the distribution is multiplied with the sampling time squared. The power spectrum of the displacement can thus be obtained from the well known power spectrum of the position [13,19]

$$\left|S_{\Delta x}(f)\right|^2 = \tau^2 f^2 \left|S_x(f)\right|^2 = 2\tau^2 f^2 \frac{D}{f^2 + f_c^2}. \quad (5)$$

Figure 2(c) shows the distribution of displacements along the x–axis and Fig. 2(b) shows the corresponding power spectrum of the displacement, both obtained through the FTMA method.

From the variance $<\Delta x^2> = 1.93 \times 10^{-4}$ μm^2 shown in Fig. 2(c), we obtain a diffusion coefficient of $D = 0.039$ μm^{2}s^{-1} in fair agreement with the value $D = 0.045$ μm^{2}s^{-1} obtained using the reference tracking method [11]. Similarly, we obtain a corner frequency of $f_c = 1.28$ Hz, from the power spectrum of the displacement, corresponding to a trap stiffness of 0.75 pN/μm in excellent agreement with the value obtained using the reference tracking method. Using the FTMA method, we are thus able to retrieve the parameters describing the motion of the trapped bead, trap stiffness and diffusion coefficient, in full agreement with the values obtained using the reference tracking method.

3.2. Tracking of fluorescent beads

To demonstrate the versatility of the FTMA method we have investigated two cases where the trapped objects are either highly irregular or the lightning conditions are changing rapidly. First, we exchange the transparent polystyrene bead with a dye imprinted bead. The bead absorbs at 580 nm and the fluorescence is centered at 605 nm. The fluorescent bead was imaged in end-view (x,y) at 100 fps and a light beam, travelling along the y-axis from a supercontinuum light source (NKT Photonics, SuperK) was used to supply 1 mW of 580 nm light on the trapped bead at $t = 0.6$ seconds. The displacements of the particle along the x-axis and the y-axis are shown in Fig. 3(b) as a function of time. The simultaneously measured fluorescence intensity is shown in Fig. 3(a). When the light source is turned on, the absorbed photons push the bead along the y-axis, but motion along the x-axis is also detected. Around $t = 0.6$ seconds when the fluorescent laser is turned on, the approximation that the spectral shape of two consecutive images should remain constant is not valid. This could contribute to the transient motion observed along the x-axis. However, the actual motion of the fluorescent sphere is a result of a non-trivial combination of the momentum transfer from the absorbed and emitted photons, bleaching of the dye, and the 3D characteristics of the optical trap. This will be described in more detail in a forthcoming paper. Tracking of the particle position with the reference method is not possible as a result of the abrupt changes in shape and illumination of the object.

#158777 - $15.00 USD Received 23 Nov 2011; revised 2 Jan 2012; accepted 2 Jan 2012; published 13 Jan 2012

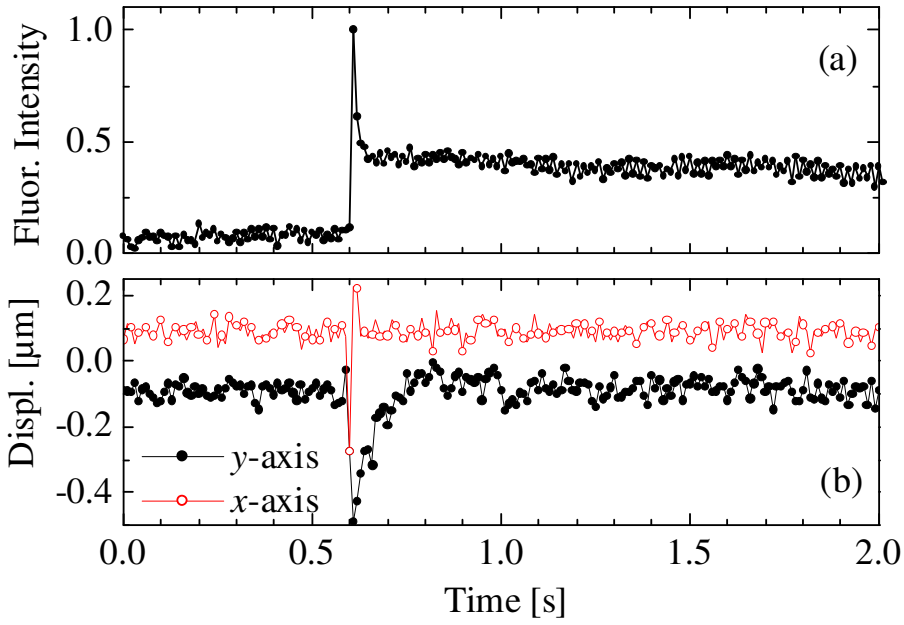

Fig. 3. (a) Normalized fluorescence intensity for an optically trapped 10 μm diameter dyed polystyrene bead as a function of time, t. At $t = 0.6$ seconds an excitation beam is turned on. (b) The corresponding particle displacement along the x-axis (red) and the y-axis (black). The curves were shift 100 nm in each direction for clarity.

3.3. Tracking of myoblast cells

As an additional example of the strength of the method, we have analyzed the motion of a trapped myoblastic cell. The C2C12 mouse myoblast cell line (American Type Culture Collection) in Dulbecco's Modified Eagles Medium was used. Polyethylene glycol(PEG) was used to minimize cell adhesion onto the glass surface. A poly(L-lysine)-*graft*-PEG (PLL-*g*-PEG) solution was employed to coat the chamber's surface since it spontaneously adsorbs onto negatively charged surfaces forming a stable polymeric monolayer [20]. The cell was trapped using a laser power of 8.1 mW in each beam, each with a focus diameter of 14 μm. The two foci were separated by 80 μm. A 30 minute video was recorded at a frame rate of 300 Hz. The image of the myoblast cells is of low quality, with non-uniform illumination of the cell and a strong and irregular background. Consequently, it was not possible to track the motion of the cell using standard image analysis. Instead, the cell was tracked using the 2D FTMA method. After a Fourier transform of the images taken, a filter was again applied to the images. The filter was composed of a DC-filter removing all wave vectors around $k_x = k_z = 0$ μm^{-1} in combination with a low pass filter that suppresses the high frequency noise in the image ($k_x = k_y > 0.5$ μm^{-1}). Subsequently, a threshold filter was used to suppress low amplitude frequencies, which are typically associated with noise. An example of the images is shown in Fig. 4, where also the DC-, low pass-, and threshold filter are indicated. From the analysis we obtain the displacement of the cell along the x- and y-directions (end-view) and the displacement along the x- and z-directions (side-view). The x-axis data from the side- and end-views show the expected correlation.

#158777 - $15.00 USD Received 23 Nov 2011; revised 2 Jan 2012; accepted 2 Jan 2012; published 13 Jan 2012

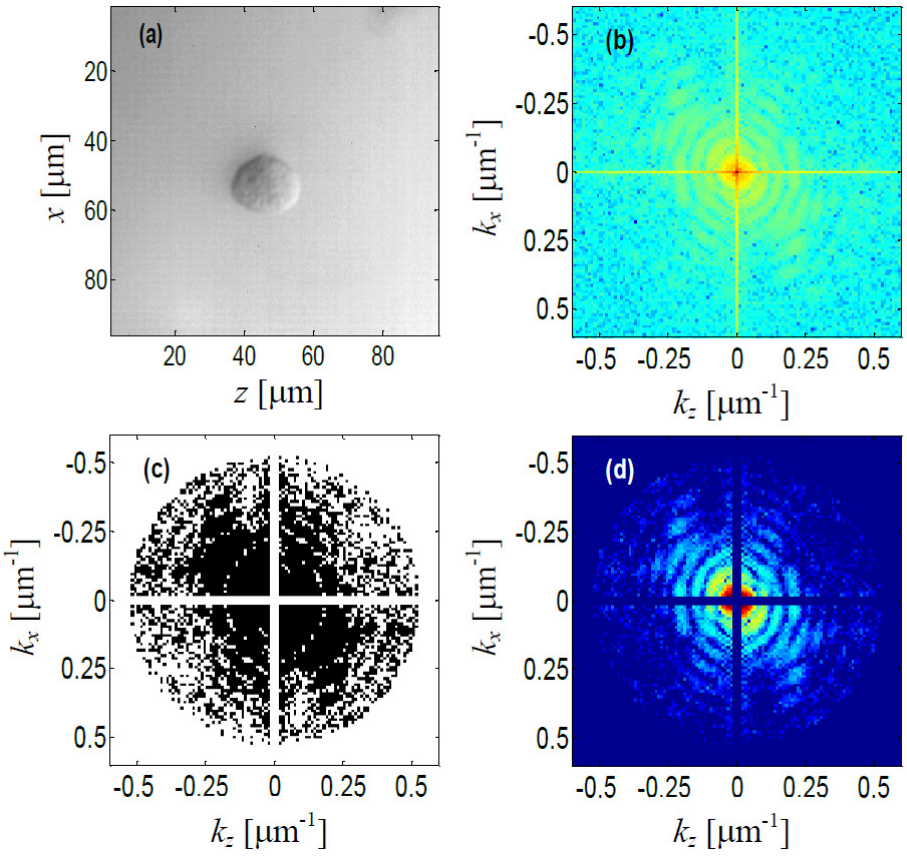

Fig. 4. (a) Image of the trapped myoblast cell indicating asymmetric illumination and background. (b) 2D Fourier transform of the image in (a). The DC background in the image results in the two lines at $k_x = k_z = 0$ μm^{-1}. (c) A 2D filter removes the DC-values around $k_x = k_z = 0$ μm^{-1} and applies a threshold in Fourier amplitude. The mask has a value of 1 in the black area and a value of 0 in the white area. (d) After application of the filtered image in (c) to the 2D Fourier transform in (b) a much clearer image of the relevant frequencies are obtained. This justifies the following use of the filter on the phase space image in order to obtain the displacements. The images of the Fourier transform amplitudes in (b) and (d) are both shown on a logarithmic scale. Red corresponds to the highest amplitude and blue to the lowest.

In Fig. 5 we show the frequency analysis of the x-axis displacement (a) and the statistical analysis (b). The distribution of the displacements is Gaussian with a variance given in Eq. (4). From the analysis we obtain a diffusion coefficient of $D = 0.015$ μm^{2}s^{-1}. This is less than half the value of the diffusion coefficient of the polystyrene sphere, in accordance with the fact that the myoblast cell is approximately twice the size of the polystyrene sphere. In the frequency analysis we determine a corner frequency along the x-axis equal to $f_c = 0.62$ Hz. From the corner frequency we obtain the trap stiffness for the x-axis, $\kappa_x = 1.07$ pN/μm.

#158777 - $15.00 USD Received 23 Nov 2011; revised 2 Jan 2012; accepted 2 Jan 2012; published 13 Jan 2012

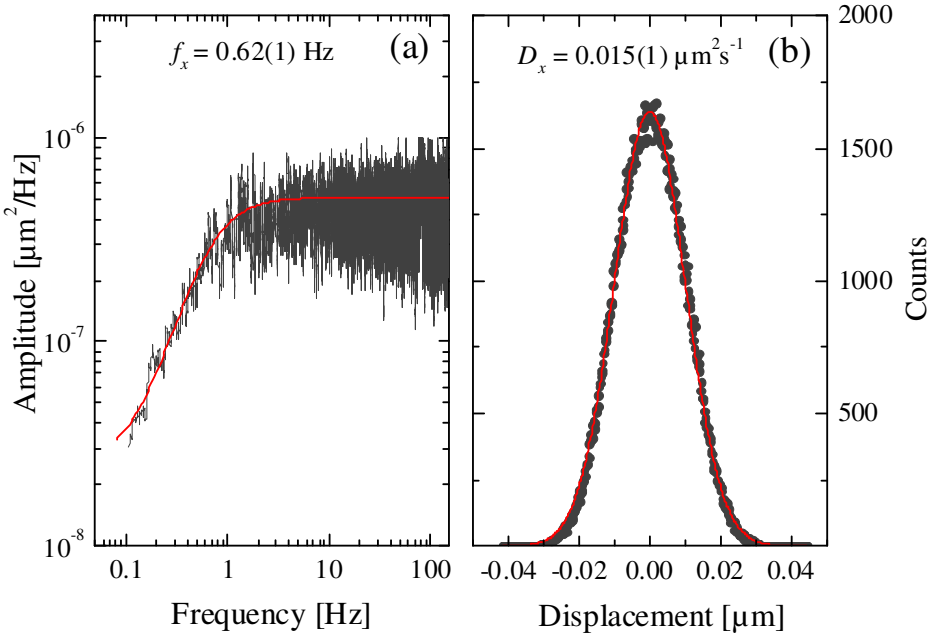

Fig. 5. (a) Frequency analysis of the *x*-displacement of the myoblast cell shown in Fig. 4. The fitted curve corresponds to a corner frequency of 0.62 Hz for the *x*-direction. Data points were averaged after fitting as in Fig. 2. (b) Distribution of the *x*-displacements obtained by tracking the motion of the myoblast cells using the FTMA method. The diffusion coefficient is D_x = 0.015(1) µm^{2}s^{-1}. Combined with the corner frequency obtained in (a) the trap stiffness can be determined to be κ_x = 1.07 pN/µm.

For the *z*-axis, the optical trap is approximately a factor of 10 weaker than for the other two axes. However, due to the low frequency noise we are therefore unable to determine the corner frequency for the *z*-axis. This is, however, a consequence of the properties of our trap rather than the FTMA method.

4. Discussion

The long timescales in our data collection is by no means a requirement of the FTMA method, but rather a requirement for properly resolving the low corner frequencies of our optical trapping system. Furthermore, the FTMA method is not restricted to trapped objects. The only requirement is that the analyzed object and the background does not change shape faster than the frame rate of the recording camera.

The FTMA method can also be employed to track multiple objects. In this work we used a simple least square fitting routine to obtain the slope of the phase plane obtained from Eq. (2) and illustrated in the inset of Fig. 1. In a more general approach, one can obtain the displacement of one, or more moving objects, by performing an inverse Fourier transform of the complex ratio of the two images given in Eq. (2) [8]

$$g(x,y) = \Im^{-1}\left[\frac{F_2(k_x,k_y)}{F_1(k_x,k_y)}\right] = \Im^{-1}\left[e^{-i(k_x\Delta x + k_y\Delta y)}\right] = \delta(x-\Delta x, y-\Delta y). \qquad (6)$$

For a single moving object, the inverse Fourier transform gives a delta function located at the displacement (Δx,Δy) as evident from Eq. (6). For multiple objects the function *g* will contain several peaks, corresponding to the motion of the center of gravity of the particles and

#158777 - $15.00 USD Received 23 Nov 2011; revised 2 Jan 2012; accepted 2 Jan 2012; published 13 Jan 2012

the motion of the individual particles relative to the center of gravity. Several factors, such as computational speed, noise, and resolution, influence the applicability of the FTMA method for multiple objects and these are presently being investigated. The FTMA method can also be used to obtain 3D motion. In the present case, where both end-view and side-view images are obtained, the method can be used to track the 3D displacement of the object. If a full 3D representation of the objects is available, the image can be transformed to spherical coordinates, and the FTMA method can be employed to detect angular displacement of the objects [8,21].

In summary, we have demonstrated a new method for tracking microscopic objects. The method is simple and straightforward to implement for arbitrary objects, as no initial definition of the image is needed. The method normalizes the shape of the object after each frame and is therefore able to efficiently track objects in cases where the illumination changes or the object itself is irregular and changing in time.

Acknowledgment

We thank the Danish Technical Scientific Research Council (FTP) for support.

#158777 - $15.00 USD Received 23 Nov 2011; revised 2 Jan 2012; accepted 2 Jan 2012; published 13 Jan 2012